

---

# Predicting Length of Stay in the Intensive Care Unit with Temporal Pointwise Convolutional Networks

---

Emma Rocheteau<sup>1</sup> Pietro Liò<sup>1</sup> Stephanie Hyland<sup>2</sup>

## Abstract

The pressure of ever-increasing patient demand and budget restrictions make hospital bed management a daily challenge for clinical staff. Most critical is the efficient allocation of resource-heavy Intensive Care Unit (ICU) beds to the patients who need life support. Central to solving this problem is knowing for how long the current set of ICU patients are likely to stay in the unit. In this work, we propose a new deep learning model based on the combination of temporal convolution and pointwise (1x1) convolution, to solve the length of stay prediction task on the eICU critical care dataset. The model – which we refer to as Temporal Pointwise Convolution (TPC) – is specifically designed to mitigate for common challenges with Electronic Health Records, such as skewness, irregular sampling and missing data. In doing so, we have achieved significant performance benefits of 18-51% (metric dependent) over the commonly used Long-Short Term Memory (LSTM) network, and the multi-head self-attention network known as the Transformer.

## 1. Introduction

In-patient length of stay (LoS) explains approximately 85 to 90% of inter-patient variation in hospital costs in the United States (Rapoport et al., 2003). Extended length of stay is associated with increased risk of contracting hospital acquired infections (Hassan et al., 2010) and mortality (Laupland et al., 2006). Hospital bed planning can help to mitigate these risks and improve patient experiences (Blom et al., 2015). This relies on data from the Electronic Health Record (EHR) system, which contains patient data such as

<sup>1</sup>Department of Computer Science and Technology, University of Cambridge, UK <sup>2</sup>Microsoft Research Cambridge, UK. Correspondence to: Emma Rocheteau <ecr38@cam.ac.uk>.

medical histories, diagnoses, medications, treatment plans, radiology images, laboratory tests and clinical notes.

At present, discharge date estimates are usually done manually by clinicians, but these rapidly become out-of-date (Nassar & Caruso, 2016) and can be unreliable<sup>1</sup>. Automated LoS forecasting could reduce the administrative burden on clinicians as well as enable more sophisticated planning strategies e.g. scheduling high-risk elective surgeries on days with more predicted availability (Gentimis et al., 2017).

In our work, we predict the remaining LoS of patients in the ICU at hourly intervals (similar to Harutyunyan et al. (2019)). Our key contributions are:

1. A new model – Temporal Pointwise Convolution (TPC) – which combines the strengths of:
  - Temporal Convolutional Layers (van den Oord et al., 2016; Kalchbrenner et al., 2016), in capturing causal dependencies across time.
  - Pointwise Convolutional Layers (Lin et al., 2013), in computing higher level features from interactions in the feature domain.

We show that these methods complement each other by extracting different information. Our model outperforms the commonly used Long-Short Term Memory (LSTM) network (Hochreiter & Schmidhuber, 1997) and the Transformer (Vaswani et al., 2017).

2. We make a case for using the mean squared logarithmic error (MSLE) loss function to train LoS models, as it helps to mitigate for positive skew in the LoS task.

Our code is available on GitHub: <https://github.com/EmmaRocheteau/eICU-LoS-prediction>.

## 2. Related Work

Owing to the centrality of time series in the EHR, LSTMs have been the most popular model for predicting LoS and have achieved state-of-the-art results (Harutyunyan et al., 2019; Sheikhalishahi et al., 2019; Rajkomar et al., 2018).

<sup>1</sup>Mak et al. (2012) found that the average error made by clinicians when predicting hospital length of stay at admission time was 3.82 days, with a standard deviation of 6.51 days.

This reflects the prominence of LSTMs in other clinical prediction tasks such as predicting in-hospital adverse events e.g. cardiac arrest (Tonekaboni et al., 2018) and acute kidney injury (Tomašev et al., 2019), forecasting diagnoses and medications (Choi et al., 2015; Lipton et al., 2015), and mortality prediction (Che et al., 2018; Harutyunyan et al., 2019; Shickel et al., 2019). The Transformer model (Vaswani et al., 2017) was originally designed for natural language processing (NLP), but it has marginally outperformed the LSTM on the LoS task (Song et al., 2018). Therefore, the LSTM and the Transformer were chosen as key baselines.

### 3. Methods

**Model Overview** We want our model to extract both trends and inter-feature relationships. Clinicians do this when assessing their patients e.g. they might check how the respiratory rate is changing over time, and they may also look at combination features e.g. the  $\text{PaO}_2/\text{FiO}_2$  ratio. We aim to extract both types of feature with our model.

**Temporal Convolution** Temporal Convolution Networks (TCNs) (van den Oord et al., 2016; Kalchbrenner et al., 2016) are 1-dimensional Convolutional Neural Networks (Fukushima, 1980) that only convolve on elements from the current timestamp or earlier. The receptive field sizes<sup>2</sup> are highly adaptable. They can be increased either by using greater dilation (spacing between filter elements), larger kernel sizes (number of filter elements) or by stacking multiple TCNs with increasing dilation, as in Wavenet (van den Oord et al., 2016) and ByteNet (Kalchbrenner et al., 2016). By contrast, RNNs can only process one time step at a time. Unlike most TCN implementations, we *do not share the weights across features* i.e. the weight sharing is only across time, like in Xception (Chollet, 2016). We hypothesised that each feature may have sufficient differences in their temporal characteristics to warrant specialised processing.

**Pointwise Convolution** Pointwise convolution (Lin et al., 2013) is also referred to as  $1 \times 1$  convolution. It is typically used to reduce the dimensions across each location on an image to allow for deeper networks (Szegedy et al., 2014). We use pointwise convolution to compute interaction features from the existing feature set at each timepoint<sup>3</sup>. Contrary to the common use case, we actually increase the channel dimension because we retain all the pointwise outputs as skip connections (see ‘Skip Connections’ below).

**Temporal Pointwise Convolution** Our model – which we refer to as Temporal Pointwise Convolution (TPC) – combines temporal and pointwise convolution in parallel.

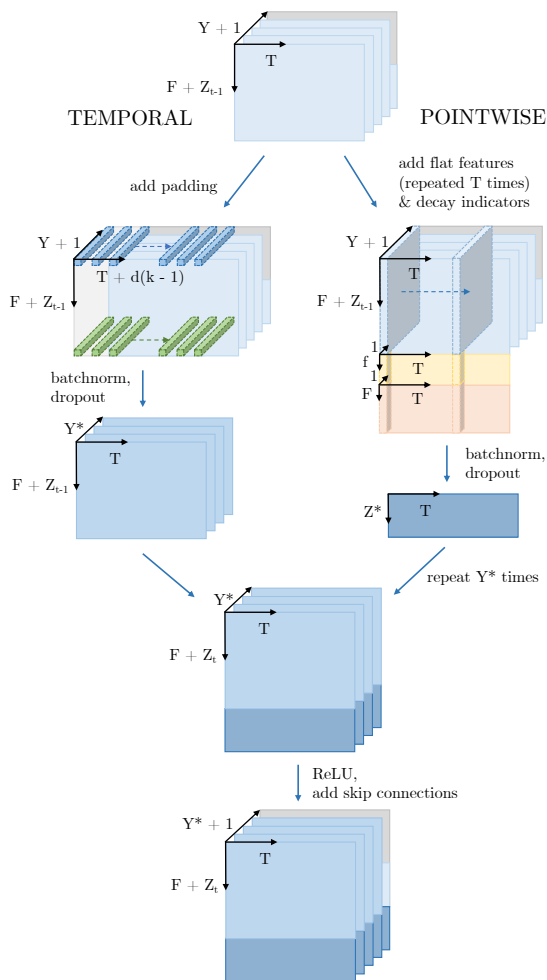


Figure 1. One layer of the TPC model.  $F$  is the number of time series features.  $T$  is the time series length.  $Y$  is the number of temporal channels per feature in the *previous* TPC layer (except for the first layer where  $Y$  is 1; decay indicators (explained under ‘Time Series’ in Appendix A.3) make up this channel).  $Z_{t-1}$  is the cumulative number of pointwise outputs from *all previous* TPC layers.  $Y^*$  and  $Z^*$  are the number of temporal channels per feature and pointwise outputs respectively in the *current* TPC layer.  $Z_t = Z_{t-1} + Z^*$ . The differently coloured temporal filters indicate independent parameters.  $d$  is the temporal dilation,  $k$  is the kernel size. Decay indicator features (Section A.3) are shown in orange,  $f$  flat features are shown in yellow. The skip connections consist of  $F$  original features (grey) and  $Z_{t+1}$  pointwise outputs (light blue). We ignore the batch dimension for clarity.

Figure 1 shows just one TPC layer, however the full model has 9 TPC layers stacked sequentially. With each successive layer, we increase the temporal dilation by 1. After processing the time series, we combine them with flat (non time-varying) features and a diagnosis embedding (Figure 2 in the Appendix shows the complete architecture). The combined features pass through a small two-layer pointwise convolution to obtain the LoS predictions. We apply an exponential and a HardTanh function (Gülçehre et al., 2016) to the model output to clip any predictions that are shorter

<sup>2</sup>‘Receptive field’ refers to the width of the convolutional filter. For TCNs this corresponds to a timespan.

<sup>3</sup>It may be helpful to conceptualise pointwise convolution as applying the same fully connected layer to each timepoint.

than 30 minutes or longer than 100 days. We use batch normalisation (Ioffe & Szegedy, 2015) and dropout (Srivastava et al., 2014) to regularise the model. The hyperparameter search methodology is described in Appendix A.6.

**Skip Connections** We propagate skip connections (He et al., 2015) to allow each TPC layer to see the original data and the pointwise outputs from previous layers. This helps the network to cope with infrequently sampled data. Suppose that a particular blood test is taken once per day (a real example is shown in Figure 3 in the Appendix). To maintain temporal resolution, the missing data is forward-filled. We convolve with increasingly dilated filters in each layer until we find the appropriate width to capture a useful trend. However, if the smaller filters in previous layers (which did not see any useful trend) have polluted the original data, learning will be harder. The skip connections are concatenated with the TPC outputs (like in DenseNet (Huang et al., 2017)) as shown in Figure 1.

**Loss Function** The remaining LoS has a positive skew (which can be seen in Appendix A.4) which makes the prediction task more challenging. We partly circumvent this problem by replacing the commonly used mean squared error (MSE) loss with mean squared *log* error (MSLE). MSLE penalises *proportional* over absolute error, which seems more reasonable when considering an error of 5 days in the context of a 2-day stay vs. a 30-day stay.

## 4. Data

We use the eICU Collaborative Research Database (Pollard et al., 2018), a multi-centre dataset collated from 208 hospitals in the United States. We selected all adult patients (>18 years) with an ICU LoS of at least 5 hours and at least one recorded observation. Our cohort had 118,534 unique patients and 146,666 ICU stays. We extracted diagnoses, flat features e.g. ethnicity, and time series including both regularly and irregularly sampled variables. Further details can be found in Appendices A.2 and A.3.

## 5. Experiments and Results

**Metrics** We report on 6 metrics for each experiment: mean absolute deviation (MAD), mean absolute percentage error (MAPE), mean squared error (MSE), mean squared log error (MSLE), coefficient of determination ( $R^2$ ) and Cohen Kappa Score. Detailed information about these metrics can be found in Appendix B.

**Baselines** We include ‘mean’ and ‘median’ models that always predict 3.50 and 1.70 days respectively (the mean and median of the training data). Our standard LSTM baseline is very similar to Sheikhalishahi et al. (2019). The channel-wise LSTM (CW LSTM) baseline consists of a set of in-

dependent LSTMs which process each feature separately (note the similarity with the TPC model). The Transformer is a multi-head self-attention model. Like the TPC model, it is not constrained to progress one timestep at a time; however, unlike TPC, it is not able to scale its receptive fields or process features independently. Implementation details can be found in Appendix A.5.

**TPC Performance** Table 1a shows that TPC outperforms all of the baseline models on every metric – particularly those that are more robust to skewness: MAPE, MSLE and Kappa. The best performing *baselines* are the Transformer and the channel-wise LSTM (CW LSTM), whose results are almost indistinguishable. Our results are highly consistent with Harutyunyan et al. (2019) (for CW LSTM) and Song et al. (2018) (for Transformers), who both found small improvements over the standard LSTM model.

**MSLE Loss Function** Table 1b shows that using the MSLE loss function rather than MSE leads to significantly improved behaviour in the TPC model, with large performance gains in MAD, MAPE, MSLE and Kappa, while conceding little in terms of MSE and  $R^2$ . The MSE results for the baselines are shown in Table 8 in the Appendix; they show a similar pattern to the TPC model.

**Ablation Studies** Table 1c shows ablations of the TPC model. We can see that the temporal-only model performs much better than the pointwise-only model, but the TPC model outperforms them both. The temporal-only model performs much better than its weight sharing ablation, suggesting that having independent parameters per feature is important for the LoS task.

We also tested the models with partial data: laboratory tests only (which are infrequently sampled), and all other variables which include vital signs, nurse observations, and automatically recorded variables. The results (shown in Appendix C.1) indicate that the TPC model is better able to exploit disparate EHR time series than the baselines. They also show that the advantage of the CW LSTM over the standard LSTM is only apparent when the model has to process different types of time series simultaneously.

## 6. Discussion

We have shown that the TPC model outperforms all baseline models on the LoS task. We believe that there are several factors contributing to its success.

The parallel architectures of the TPC model are designed to extract different information: trends from the temporal component and feature interactions from the pointwise component. Their contributions are complementary; however, we stress that the temporal convolutions are more important.

Table 1. Performance of the TPC model compared to the baselines (a) and ablation studies (b) and (c). Unless otherwise specified, the loss function is MSLE. For the first four metrics, lower is better. The error margins are 95% confidence intervals (CIs) calculated over 10 runs. (a) shows the baseline comparisons. (b) compares the effect of the loss function on the TPC model. (c) shows ablations of the TPC model. WS refers to weight sharing between the features. The best results are highlighted in blue. If an upper CI exceeds the lower CI of the best result, then it is highlighted in light blue. Note that the TPC result has been repeated for ease of comparison.

	Model	MAD	MAPE	MSE	MSLE	R <sup>2</sup>	Kappa
(a)	Mean	3.21	395.7	29.5	2.87	0.00	0.00
	Median	2.76	184.4	32.6	2.15	-0.11	0.00
	LSTM	2.39±0.00	118.2±1.1	26.9±0.1	1.47±0.01	0.09±0.00	0.28±0.00
	CW LSTM	2.37±0.00	114.5±0.4	26.6±0.1	1.43±0.00	0.10±0.00	0.30±0.00
	Transformer	2.36±0.00	114.1±0.6	26.7±0.1	1.43±0.00	0.09±0.00	0.30±0.00
	TPC	<b>1.78±0.02</b>	<b>63.5±4.3</b>	<b>21.7±0.5</b>	<b>0.70±0.03</b>	<b>0.27±0.02</b>	<b>0.58±0.01</b>
(b)	TPC (MSLE)	<b>1.78±0.02</b>	<b>63.5±4.3</b>	<b>21.7±0.5</b>	<b>0.70±0.03</b>	<b>0.27±0.02</b>	<b>0.58±0.01</b>
	TPC (MSE)	2.21±0.02	154.3±10.1	<b>21.6±0.2</b>	1.80±0.10	<b>0.27±0.01</b>	0.47±0.01
(c)	TPC	<b>1.78±0.02</b>	<b>63.5±3.8</b>	<b>21.8±0.5</b>	<b>0.71±0.03</b>	<b>0.26±0.02</b>	<b>0.58±0.01</b>
	Pointwise-only	2.68±0.15	137.8±16.4	29.8±2.9	1.60±0.03	-0.01±0.10	0.38±0.01
	Temporal-only	1.91±0.01	71.2±1.1	23.1±0.2	0.86±0.01	0.22±0.01	0.52±0.01
	Temporal-only (WS)	2.34±0.01	116.0±1.2	26.5±0.2	1.40±0.01	0.10±0.01	0.31±0.00

The temporal-only model betters its most direct comparison, the CW LSTM, on all metrics<sup>4</sup>. To explain this, we can consider how the information flows through the model. The temporal-only model can directly step across large time gaps, whereas the CW LSTM is forced to progress one timestep at a time. This gives the CW LSTM the comparatively harder task of remembering information across a noisy EHR with distracting signals of varying frequency. In addition, the temporal-only model can easily tune its receptive fields for optimal processing of each feature thanks to the skip connections (not present in the CW LSTM).

The difference in performance between the temporal-only model with and without weight sharing provides strong evidence that assigning independent parameters to each feature is important for the LoS task. Some EHR time series are irregularly and sparsely sampled, and can exhibit considerable variability in the temporal frequencies within the underlying data (this is evident in Figure 3 in the Appendix). This presents a difficult challenge for any model, especially if it is constrained to learn one set of parameters to suit all features. The relative success of the CW LSTM over the standard LSTM when processing *disparate* time series – but not similar – also lends weight to this theory.

However, the assignment of independent parameters to each feature does not explain all the successes of the TPC model e.g. the TPC processes *disparate* time series better than the CW LSTM. We need to consider that *periodicity* is a key

<sup>4</sup>Theoretically they are well matched because they both have feature-specific parameters and they are unable to compute cross-feature interactions until the final layers of the model (which are identical as shown in Figure 2 in the Appendix).

property of EHR data<sup>5</sup>. The temporal component of the TPC model has an inherent periodic structure which makes it much easier to learn EHR trends. By comparison, a single attention head in the Transformer model does not look at timepoints a fixed distance apart, but can take an arbitrary form. This is helpful for NLP applications but not for EHRs.

Finally, we reiterate that using MSLE loss instead of MSE greatly mitigates for positive skew in the LoS task, although this is not model-specific (all of the baselines benefit from MSLE). This demonstrates that careful consideration of the task – as well as the data and model – is an important step towards building useful tools for healthcare providers.

## 7. Conclusion

The TPC model is well-equipped to analyse EHR time series containing different frequencies, missingness and sparse sampling. We believe that the following aspects contribute the most to its success:

- The combination of two complementary architectures that are able to extract different features, both of which are important for patient assessment.
- The ability to step directly over large gaps in time.
- The capacity to specialise processing to each feature (including the freedom to select the appropriate receptive field size for each).
- The rigid spacing of the temporal filters, making it easy to derive trends in the EHR.

<sup>5</sup>This is true both in sampling patterns and in the underlying biological functions e.g. responses to medication schedules.

From a clinical perspective, we have contributed to the advancement of LoS prediction models, a prerequisite for automated bed management tools. From a computational perspective, we have provided key insights for retrospective EHR studies, particularly where LSTMs are the currently model of choice.

## Acknowledgements

The authors would like to thank Alex Campbell, Petar Veličković, and Ari Ercole for helpful discussions and advice. We would also like to thank Louis-Pascal Xhonneux, Cătălina Cangea and Nikola Simidjievski for their help in reviewing the manuscript. Finally we thank the Armstrong Fund, the Frank Edward Elmore Fund, and the School of Clinical Medicine at the University of Cambridge for their generous funding.

## References

- Blom, M. C., Erwander, K., Gustafsson, L. M., Landin-Olsson, M., Jonsson, F., and Ivarsson, K. The Probability of Readmission within 30 days of Hospital Discharge is Positively Associated with Inpatient Bed Occupancy at Discharge A Retrospective Cohort Study. In *BMC Emergency Medicine*, 2015.
- Che, Z., Purushotham, S., Cho, K., Sontag, D., and Liu, Y. Recurrent Neural Networks for Multivariate Time Series with Missing Values. *Scientific Reports*, 8(1):6085, 2018.
- Choi, E., Bahadori, M. T., Schuetz, A., Stewart, W. F., and Sun, J. Doctor AI: Predicting Clinical Events via Recurrent Neural Networks. *JMLR workshop and conference proceedings*, 56:301–318, 2015.
- Chollet, F. Xception: Deep Learning with Depthwise Separable Convolutions. *CoRR*, abs/1610.02357, 2016.
- Cohen, J. A Coefficient of Agreement for Nominal Scales. *Educational and Psychological Measurement*, 20(1):37–46, 1960.
- De Silva, T. S., MacDonald, D., Paterson, G., Sikdar, K. C., and Cochrane, B. Systematized Nomenclature of Medicine Clinical Terms (SNOMED CT) to Represent Computed Tomography Procedures. *Comput. Methods Prog. Biomed.*, 101(3):324329, 2011.
- Elixhauser, A., Steiner, C., and Palmer, L. Clinical Classifications Software, 2015.
- Fukushima, K. Neocognitron: A Self-Organizing Neural Network Model for a Mechanism of Pattern Recognition Unaffected by Shift in Position. *Biological Cybernetics*, 36(4):193–202, 1980.
- Gentimis, T., Alnaser, A. J., Durante, A., Cook, K., and Steele, R. Predicting Hospital Length of Stay Using Neural Networks on MIMIC III Data. In *2017 IEEE 15th Intl Conf on Dependable, Autonomic and Secure Computing*, pp. 1194–1201, 2017.
- Gülçehre, Ç., Moczulski, M., Denil, M., and Bengio, Y. Noisy Activation Functions. *CoRR*, abs/1603.00391, 2016.
- Harutyunyan, H., Khachatrian, H., Kale, D. C., Ver Steeg, G., and Galstyan, A. Multitask Learning and Benchmarking with Clinical Time Series Data. *Scientific Data*, 6(96), 2019.
- Hassan, M., Tuckman, H., Patrick, R., Kountz, D., and Kohn, J. Hospital Length of Stay and Probability of Acquiring Infection. *International Journal of Pharmaceutical and Healthcare Marketing*, 4:324–338, 2010.
- He, K., Zhang, X., Ren, S., and Sun, J. Deep Residual Learning for Image Recognition. *CoRR*, abs/1512.03385, 2015.
- Hochreiter, S. and Schmidhuber, J. Long Short-Term Memory. *Neural computation*, 9(8):1735–1780, 1997.
- Huang, G., Liu, Z., van der Maaten, L., and Weinberger, K. Q. Densely connected convolutional networks. In *Proceedings of the IEEE Conference on Computer Vision and Pattern Recognition*, 2017.
- Ioffe, S. and Szegedy, C. Batch normalization: Accelerating deep network training by reducing internal covariate shift. In *Proceedings of the 32nd International Conference on International Conference on Machine Learning - Volume 37, ICML'15*, pp. 448–456. JMLR, 2015.
- Kalchbrenner, N., Espeholt, L., Simonyan, K., van den Oord, A., Graves, A., and Kavukcuoglu, K. Neural Machine Translation in Linear Time. *CoRR*, abs/1610.10099, 2016.
- Kingma, D. P. and Ba, J. Adam: A method for stochastic optimization. *CoRR*, abs/1412.6980, 2014.
- Laupland, K. B., Kirkpatrick, A. W., Kortbeek, J. B., and Zuege, D. J. Long-term Mortality Outcome Associated With Prolonged Admission to the ICU. *Chest*, 129(4): 954 – 959, 2006.
- Lin, M., Chen, Q., and Yan, S. Network In Network, 2013.
- Lipton, Z. C., Kale, D. C., Elkan, C., and Wetzel, R. C. Learning to Diagnose with LSTM Recurrent Neural Networks. *CoRR*, abs/1511.03677, 2015.
- Mak, G., Grant, W. D., McKenzie, J. C., and McCabe, J. B. Physicians’ Ability to Predict Hospital Length of Stay for Patients Admitted to the Hospital from the Emergency Department. In *Emergency medicine international*, 2012.



- Nassar, A. P. and Caruso, P. ICU Physicians are Unable to Accurately Predict Length of Stay at Admission: A Prospective Study. *Journal of the International Society for Quality in Health Care*, 28 1:99–103, 2016.
- NHS Digital. DCB0084: OPCS-4.9 Requirements Specification, 2019.
- Paszke, A., Gross, S., Massa, F., et al. PyTorch: An Imperative Style, High-Performance Deep Learning Library. In *Advances in Neural Information Processing Systems 32*, pp. 8024–8035. Curran Associates, Inc., 2019.
- Pollard, T. J., Johnson, A. E. W., Raffa, J. D., Celi, L. A., Mark, R. G., and Badawi, O. The eICU Collaborative Research Database, A Freely Available Multi-Center Database for Critical Care Research. *Scientific Data*, 5 (1):180178, 2018.
- Rajkomar, A., Oren, E., Chen, K., et al. Scalable and Accurate Deep Learning with Electronic Health Records. In *npj Digital Medicine*, 2018.
- Rapoport, J., Teres, D., Zhao, Y., and Lemeshow, S. Length of Stay Data as a Guide to Hospital Economic Performance for ICU Patients. *Medical Care*, 41:386–397, 2003.
- Sheikhalishahi, S., Balaraman, V., and Osmani, V. Benchmarking Machine Learning Models on eICU Critical Care Dataset, 2019.
- Shickel, B., Loftus, T. J., Adhikari, L., Ozrazgat-Baslanti, T., Bihorac, A., and Rashidi, P. DeepSOFA: A Continuous Acuity Score for Critically Ill Patients using Clinically Interpretable Deep Learning. In *Scientific Reports*, 2019.
- Song, H., Rajan, D., Thiagarajan, J., and Spanias, A. Attend and Diagnose: Clinical Time Series Analysis using Attention Models. In *32nd AAAI Conference on Artificial Intelligence, AAAI 2018*, pp. 4091–4098. AAAI press, 2018.
- Srivastava, N., Hinton, G., Krizhevsky, A., Sutskever, I., and Salakhutdinov, R. Dropout: A Simple Way to Prevent Neural Networks from Overfitting. *Journal of Machine Learning Research*, 15:1929–1958, 2014.
- Szegedy, C., Liu, W., Jia, Y., Sermanet, P., Reed, S. E., Anguelov, D., Erhan, D., Vanhoucke, V., and Rabinovich, A. Going Deeper with Convolutions. *CoRR*, abs/1409.4842, 2014.
- Tomašev, N., Glorot, X., Rae, J. W., et al. A Clinically Applicable Approach to Continuous Prediction of Future Acute Kidney Injury. *Nature*, 572(7767):116–119, 2019.
- Tonekaboni, S., Mazwi, M., Laussen, P., Eytan, D., Greer, R., Goodfellow, S. D., Goodwin, A., Brudno, M., and Goldenberg, A. Prediction of Cardiac Arrest from Physiological Signals in the Pediatric ICU. In *MLHC*, 2018.
- van den Oord, A., Dieleman, S., Zen, H., Simonyan, K., Vinyals, O., Graves, A., Kalchbrenner, N., Senior, A. W., and Kavukcuoglu, K. WaveNet: A Generative Model for Raw Audio. *CoRR*, abs/1609.03499, 2016.
- Vaswani, A., Shazeer, N., Parmar, N., Uszkoreit, J., Jones, L., Gomez, A. N., Kaiser, L., and Polosukhin, I. Attention is all you need. 2017.
- World Health Organisation. *ICD-10: International Statistical Classification of Diseases and Related Health Problems*, volume 10th Revision. World Health Organisation, 2011.
- Zimmerer, D., Petersen, J., Khler, G., Wasserthal, J., Adler, T., Wirkert, S., and Ross, T. trixi - Training and Retrospective Insight eXperiment Infrastructure. <https://github.com/MIC-DKFZ/trixi>, 2017.

## A. Implementation Details

### A.1. Model Overview

Figure 2 shows the full architecture. The exponential function is intended to help to circumvent a common issue seen in previous models (e.g. Harutyunyan et al. (2019), as they struggle to produce predictions over the full range of length of stays). It effectively allows the upstream network to model  $\log(\text{LoS})$  instead of LoS. This distribution is much closer to a Gaussian distribution than the remaining LoS distribution.

We apply a HardTanh function (Gülçehre et al., 2016) to the output to clip any predictions that are smaller than 30 minutes or larger than 100 days, which protects against inflated loss values:

$$\text{HardTanh}(x) = \begin{cases} 100, & \text{if } x > 100, \\ \frac{1}{48}, & \text{if } x < \frac{1}{48}, \\ x, & \text{otherwise.} \end{cases}$$

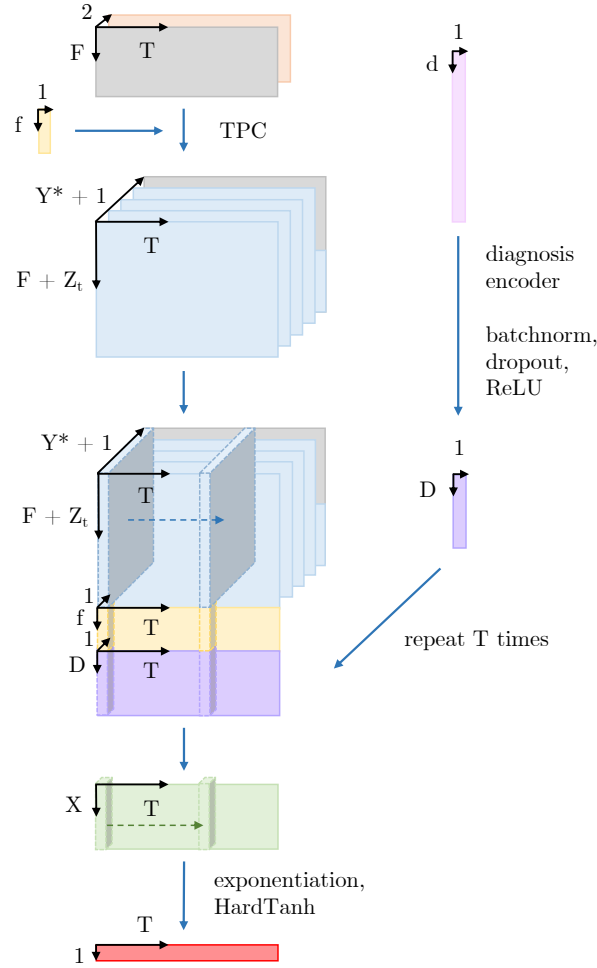


Figure 2. Overview of the framework used for the TPC model and the baselines.  $F$ ,  $T$ ,  $Y^*$ ,  $Z^*$ ,  $Z_t$  and  $f$  are defined in the caption to Figure 1. The original time series (grey) along with the decay indicators (orange) (explained under ‘Time Series’ in Section A.3) are processed by  $n$  TPC layers. If a baseline model were used instead of TPC, the time series output dimensions would be  $M \times T$ , where  $M$  is the LSTM hidden size or  $d_{model}$  in the Transformer (this is in place of the light blue and grey output in the TPC model). The diagnoses,  $d$ , are embedded by a diagnosis encoder – a single fully connected layer of size  $D$ . The time series (blue and grey), diagnosis embedding (purple) and flat features (yellow) are concatenated along the feature axis, and a two-layer pointwise convolution is applied to obtain the final predictions (red).

## A.2. Feature Selection

We selected time series variables from the following tables: *lab*, *nursecharting*, *respiratorycharting*, *vitalperiodic* and *vitalaperiodic*. We used a semi-automatic process for feature selection. To be included, the variable had to be present in at least 12.5% of patient stays, or 25% of stays for *lab* variables. The *lab* table contains a much larger number of variables than the other tables, and they tend to be sparsely sampled (once per day or less). We extracted diagnoses from the *pasthistory*, *admissiondx* and *diagnoses* tables, and 17 flat (non time-varying) features from the *patient*, *apachepatientresult* and *hospital* tables (see Table 2).

## A.3. Feature Pre-processing

**Flat Features** Discrete and continuous variables were scaled to the interval  $[-1, 1]$ , using the 5th and 95th percentiles as the boundaries, and absolute cut offs were placed at  $[-4, 4]$ . This was to protect against large or erroneous inputs, while avoiding assumptions about the variable distributions. Binary variables were coded as 1 and 0. Categorical variables were converted to one-hot encodings.

Table 2. Flat features used in the model. Age >89, Null Height and Null Weight were added as indicator variables to indicate when the age was more than 89 but has been capped, and when the height or weight were missing and have been imputed with the mean value.

Feature	Type	Source Table
Gender	Binary	patient
Age	Discrete	patient
Hour of Admission	Discrete	patient
Height	Continuous	patient
Weight	Continuous	patient
Ethnicity	Categorical	patient
Unit Type	Categorical	patient
Unit Admit Source	Categorical	patient
Unit Visit Number	Categorical	patient
Unit Stay Type	Categorical	patient
Num Beds Category	Categorical	hospital
Region	Categorical	hospital
Teaching Status	Binary	hospital
Physician Speciality	Categorical	apachepatientresult
Age >89	Binary	
Null Height	Binary	
Null Weight	Binary	

**Time Series** For each admission, 87 time-varying features (including hour of the day and time since admission) were extracted from each hour of the ICU visit, and up to 24 hours before the ICU visit. The variables were processed in the same manner as the flat features. In general, the sampling is very irregular, so the data was re-sampled according to one hour intervals. Where there is missingness, we forward-fill to bridge the gaps in the data<sup>6</sup>. After forward-filling is complete, any data recorded before the ICU admission is removed. To inform the model about where the data is stale, we add a ‘decay indicator’ to each feature to track how long it has been since a genuine observation was recorded. The decay is calculated as  $0.75^t$ , where  $t$  is the time since the last recording. If it is up to date, decay is 1, and if it cannot be forward-filled, decay is 0. This is similar in spirit to the masking used by Che et al. (2018). A real example is shown in Figure 3.

**Diagnoses** Like many EHRs, diagnosis coding in eICU is hierarchical. At the lowest level they can be quite specific e.g. “neurologic | disorders of vasculature | stroke | hemorrhagic stroke | subarachnoid hemorrhage | with vasospasm”. To maintain the hierarchical structure within a flat vector, we assigned separate features to each hierarchical level and use binary encoding. This produces a vector of size 4,436 with an average sparsity of 99.5% (only 0.5% of the data is positive). We

<sup>6</sup>This is preferable to interpolating between the data points because in realistic scenarios the clinician would only have the most recent value and its timestamp.



## TPC Networks for LoS Prediction in the ICU

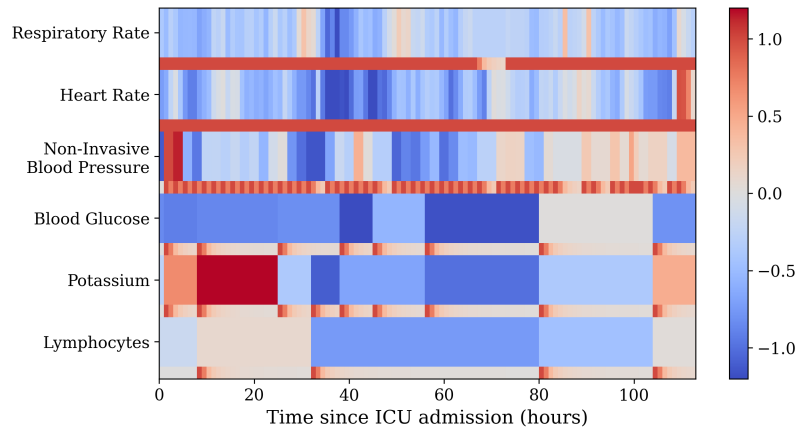


Figure 3. A selection of variables from one patient (after pre-processing). The colour scale indicates the value of the feature. Each feature is accompanied by its decay indicator (narrow bar underneath). Blood Glucose, Potassium and Lymphocytes are all laboratory tests. These are performed approximately once per day but we can see that the frequency is irregular. Non-invasive blood pressure is a variable that is recorded by the nurse. The sampling frequency is around 2 hours and is quite consistent. Respiratory Rate and Heart Rate are vital signs that are automatically logged at regular intervals.

apply a 1% prevalence cut-off on all these features to reduce the size of the vector to 293 and the average sparsity to 93.3%. If a disease does not make the cut-off for inclusion, it is still included via any parent classes that do make the cut-off (in the above example we record everything up to “subarachnoid hemorrhage”). We only included diagnoses that were recorded before the 5th hour in the ICU, to avoid leakage from the future.

Many diagnostic and interventional coding systems are hierarchical in nature: ICD-10 classification (World Health Organisation, 2011), Clinical Classifications Software (Elixhauser et al., 2015), SNOMED CT (De Silva et al., 2011) and OPCS Classification of Interventions and Procedures (NHS Digital, 2019), so this technique is generalisable to other coding systems present in EHRs.

After pre-processing, the data were divided such that 70% of patients were used for training, 15% for validation and 15% for testing.

### A.4. Remaining Length of Stay Task

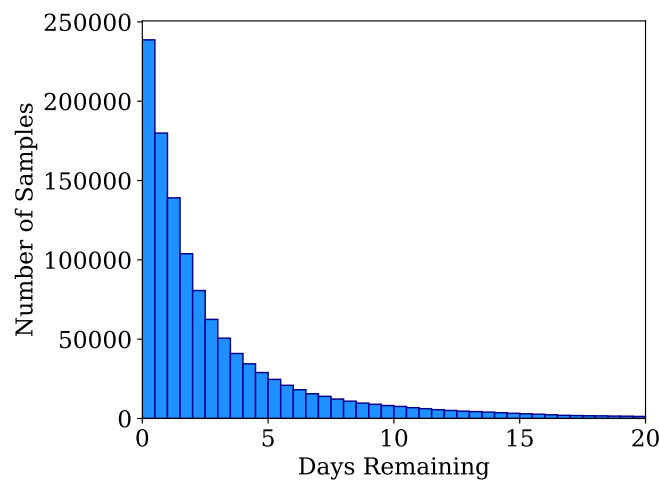


Figure 4. Remaining length of stay of the test set. The mean and median are 3.47 and 1.67 days respectively. The maximum LoS is 98.6 days, but for clarity the x axis has been limited to 20 days.

We assign a remaining LoS target to each hour of the stay, beginning 5 hours after admission to the ICU and ending when

the patient dies or is discharged. The remaining LoS is calculated by subtracting the time elapsed in the ICU from the total LoS. We only train on data within the first 14 days of any patient’s stay to protect against batches becoming overly long and slowing down training. This cut-off applies to 2.4% of patient stays, but it does *not* affect their maximum remaining length of stay values because these appear within the first 14 days. The remaining LoS distribution is shown in Figure 4.

### A.5. Baselines

A certain level of performance is achievable ‘for free’ just by predicting values that are close to the mean or median LoS (3.50 and 1.70 days respectively). We include these static models as elemental baselines. Our ‘stronger’ baselines are a two-layer *Long-Short Term Memory* network (LSTM) (Hochreiter & Schmidhuber, 1997), a two-layer channel-wise LSTM, and a Transformer encoder network (Vaswani et al., 2017) (see Section A.6 for their hyperparameters).

Our standard LSTM baseline is very similar to the one used in a recent eICU benchmark paper including LoS prediction (Sheikhalishahi et al., 2019). The channel-wise LSTM (CW LSTM) consists of a set of independent LSTMs that process each feature separately. Like our TPC model, the CW LSTM has independent parameters dedicated to each time series feature. In theory, it should be able to cope better with irregular sampling and varying frequencies in the data, but it may be hindered by the inability to compute cross-feature interactions along the way. Harutyunyan et al. (2019) found that they performed better than the standard LSTM.

The Transformer was shown to perform marginally better than the standard LSTM when predicting LoS (Song et al., 2018). It is a multi-head self-attention model, originally designed for sequence-to-sequence tasks in natural language processing. It consists of both an encoder and decoder, however we only use the former because the LoS task is regression. Our implementation is the same as the original encoder in Vaswani et al. (2017), except that we add temporal masking to impose causality<sup>7</sup>, and we omit the positional encodings because they were not helpful for the LoS task (see Table 5). Hypothetically, the Transformer shares an advantage with TPC in that it is not constrained to progress one timestep at a time. However, it is not able to scale its receptive fields in the same way as TPC and it does not have independent parameters per feature.

In all network baselines, the data (including decay indicators) and the non-time series components of the models were the same as in TPC (Figure 2).

### A.6. Hyperparameter Search

Our model and its baselines have hyperparameters that can broadly be split into three categories: time series specific, non-time series specific and global parameters (shown in more detail in Tables 3, 4 and 5). The hyperparameter search ranges have been included in Table 6. First, we ran 25 randomly sampled hyperparameter trials on the TPC model to decide the non-time series specific parameters (diagnosis embedding size, final fully connected layer size, batch normalisation strategy and dropout rate) keeping all other parameters fixed. These parameters then remained fixed for all the models which share their non-time series specific architecture. We ran 50 hyperparameter trials to optimise the remaining parameters for the TPC, standard LSTM, and Transformer models. To train the channel-wise LSTM and the temporal model with weight sharing, we ran a further 10 trials to re-optimize the hidden size (8 per feature) and number of temporal channels (32 channels shared across all features) respectively. For all other ablation studies and variations of each model, we kept the same hyperparameters where applicable (see Table 1 for a full list of all the models). The number of epochs was determined by selecting the best validation performance from a model trained over 50 epochs. This was different for each model: 8 for LSTM, 30 for CW LSTM, and 15 for the Transformer and TPC models. We noted that the best LSTM hyperparameters were similar to that found in Sheikhalishahi et al. (2019). We used trixi to structure our experiments and easily compare different hyperparameter choices (Zimmerer et al., 2017). All deep learning methods were implemented in PyTorch (Paszke et al., 2019) and were optimised using Adam (Kingma & Ba, 2014).

<sup>7</sup>The processing of each timepoint can only depend on current or earlier positions in the sequence

Table 3. The TPC model has 11 hyperparameters (Main Dropout and Batch Normalisation have been repeated in the table because they apply to multiple parts of the model). We allowed the model to optimise a custom dropout rate for the temporal convolutions because they have fewer parameters and might need less regularisation than the rest of the model. The best hyperparameter values are shown in brackets. Hyperparameters marked with \* were fixed across all of the models.

TPC Specific		Non-TPC Specific	Global Parameters
Temporal Specific	Pointwise Specific		
Temp. Channels (12)	Point. Channels (13)	Diag. Embedding Size* (64)	Batch Size (32)
Temp. Dropout (0.05)	Main Dropout* (0.45)	Main Dropout* (0.45)	Learning Rate (0.00226)
Kernel Size (4)		Final FC Layer Size* (17)	
	Batch Normalisation* (True)	Batch Normalisation* (True)	
	No. TPC Layers (9)		

Table 4. The LSTM model has 9 hyperparameters. We allowed the model to optimise a custom dropout rate for the LSTM layers. Note that batch normalisation is not applicable to the LSTM layers. The best hyperparameter values are shown in brackets. Hyperparameters marked with \* were fixed across all of the models.

LSTM Specific	Non-LSTM Specific	Global Parameters
Hidden State (128)	Diag. Embedding Size* (64)	Batch Size (512)
LSTM Dropout (0.2)	Main Dropout* (0.45)	Learning Rate (0.00129)
No. LSTM Layers (2)	Final FC Layer Size* (17)	
	Batch Normalisation* (True)	

Table 5. The Transformer model has 12 hyperparameters. We allowed the model to optimise a custom dropout rate for the Transformer layers. The positional encoding hyperparameter is binary; it determines whether or not we used the original positional encodings proposed by Vaswani et al. (2017). They were not found to be helpful (perhaps because we already have a feature to indicate the position in the time series (Section A.3)). Note that batch normalisation is not applicable to the Transformer layers (the default implementation uses layer normalisation). The best hyperparameter values are shown in brackets. Hyperparameters marked with \* were fixed across all of the models.

Transformer Specific	Non-Transformer Specific	Global Parameters
No. Attention Heads (2)	Diag. Embedding Size* (64)	Batch Size (32)
Feedforward Size (256)	Main Dropout* (0.45)	Learning Rate (0.00017)
$d_{model}$ (16)	Final FC Layer Size* (17)	
Positional Encoding (False)	Batch Normalisation* (True)	
Transformer Dropout (0)		
No. Transformer Layers (6)		

Table 6. Hyperparameter Search Ranges. We took a random sample from each range and converted to an integer if necessary. For the kernel sizes (not shown in the table) the range was dependent on the number of TPC layers selected (because large kernel sizes combined with a large number of layers can have an inappropriately wide range as the dilation factor increases per layer). In general the range of kernel sizes was around 2-5 (but it could be up to 10 for small numbers of TPC Layers).

Hyperparameter	Lower	Upper	Scale
Batch Size	4	512	$\log_2$
Dropout Rate (all)	0	0.5	Linear
Learning Rate	0.0001	0.01	$\log_{10}$
Batch Normalisation	True	False	
Positional Encoding	True	False	
Diagnosis Embedding Size	16	64	$\log_2$
Final FC Layer Size	16	64	$\log_2$
Channel-Wise LSTM Hidden State Size	4	16	$\log_2$
Point. Channels	4	16	$\log_2$
Temp. Channels	4	16	$\log_2$
Temp. Channels (weight sharing)	16	64	$\log_2$
LSTM Hidden State Size	16	256	$\log_2$
$d_{model}$	16	256	$\log_2$
Feedforward Size	16	256	$\log_2$
No. Attention Heads	2	16	$\log_2$
No. TPC Layers	1	12	Linear
No. LSTM Layers	1	4	Linear
No. Transformer Layers	1	10	Linear

## B. Evaluation Metrics

The metrics we use are: mean absolute deviation (MAD), mean absolute percentage error (MAPE), mean squared error (MSE), mean squared loss error (MSLE), coefficient of determination ( $R^2$ ) and Cohen Kappa Score. We use 6 different metrics because there is a risk that bad models can ‘cheat’ particular metrics just by virtue of being close to the mean or median value, or by not predicting long length of stays. This is not what we want in a bed management model, because long length of stays are disproportionately important due to their lasting effect on occupancy.

We have modified the MAPE metric slightly so that very small true LoS values do not produce unbounded MAPE values. We place a 4 hour lower bound on the divisor i.e.

$$\text{Absolute Percentage Error} = \left| \frac{y_{true} - y_{pred}}{\max(y_{true}, \frac{4}{24})} \right| * 100$$

MAD and MAPE are improved by centering predictions on the median. Likewise, MSE and  $R^2$  are bettered by centering predictions around the mean. They are more affected by the skew. MSLE is a good metric for this task, indeed, it is the loss function in most experiments, but is less readily-interpretable than some of the other measures. Cohen’s linear weighted Kappa Score (Cohen, 1960) is intended for ordered classification tasks rather than regression, but it can effectively mitigate for skew if the bins are chosen well. It has previously provided useful insights in Harutyunyan et al. (2019), so we use the same LoS bins: 0-1, 1-2, 2-3, 3-4, 4-5, 5-6, 6-7, 7-8, 8-14, and 14+ days. As a classification measure, it will treat everything falling within the same classification bin as equal, so it is fundamentally a coarser measure than the other metrics.

To illustrate the importance of using multiple metrics, consider that the mean and median models are in some sense equally poor (neither has learned anything meaningful for our purposes). Nevertheless, the median model is able to better exploit the MAD, MAPE and MSLE metrics, and the mean model fares better with MSE, but the Kappa score betrays them both. A good model will perform well across all of the metrics.

## C. Additional Investigations

### C.1. Time Series Ablation

Table 7. Performance of the TPC model and its baselines when only some of the time series are included. The indicator ‘(labs)’ means that the model has been trained exclusively on laboratory tests, ‘(other)’ refers to everything except labs: vital signs, nurse observations and machine logged variables. The metrics are defined in Section B. The colour scheme and confidence interval calculation is described in the legend to Table 1. The percentage impairment when compared to the complete dataset is shown in grey underneath the absolute values. They are calculated with respect to the best value for the metric: 0 for MAD, MAPE, MSE and MSLE, and 1 for  $R^2$  and Kappa. A large percentage impairment means that the model does much better with complete data i.e. it has a high ‘percentage gain’ from the combination of both data types compared to the ablation case.

Model	MAD	MAPE	MSE	MSLE	$R^2$	Kappa
LSTM	<b>2.39±0.00</b>	<b>118.2±1.1</b>	<b>26.9±0.1</b>	<b>1.47±0.01</b>	<b>0.09±0.00</b>	<b>0.28±0.00</b>
LSTM (labs)	2.43±0.00	123.8±1.2	27.3±0.1	1.57±0.00	0.08±0.00	0.27±0.00
	(-1.7%)	(-4.7%)	(-1.5%)	(-6.8%)	(-1.1%)	(-1.4%)
LSTM (other)	2.41±0.00	120.2±0.7	27.3±0.1	1.49±0.00	0.07±0.00	0.27±0.00
	(-0.8%)	(-1.7%)	(-1.5%)	(-1.4%)	(-2.2%)	(-1.4%)
CW LSTM	<b>2.37±0.00</b>	<b>114.5±0.4</b>	<b>26.6±0.1</b>	<b>1.43±0.00</b>	<b>0.10±0.00</b>	<b>0.30±0.00</b>
CW LSTM (labs)	2.42±0.00	124.4±0.7	27.0±0.1	1.57±0.00	0.08±0.00	0.28±0.00
	(-2.1%)	(-8.6%)	(-1.5%)	(-9.8%)	(-2.2%)	(-2.9%)
CW LSTM (other)	2.41±0.00	120.6±0.8	27.1±0.1	1.51±0.00	0.08±0.00	0.29±0.00
	(-1.7%)	(-5.3%)	(-1.9%)	(-5.6%)	(-2.2%)	(-1.4%)
Transformer	<b>2.36±0.00</b>	<b>114.1±0.6</b>	<b>26.7±0.1</b>	<b>1.43±0.00</b>	<b>0.09±0.00</b>	<b>0.30±0.00</b>
Transformer (labs)	2.42±0.00	121.0±0.7	27.3±0.1	1.56±0.00	0.07±0.00	0.27±0.00
	(-2.5%)	(-6.0%)	(-2.2%)	(-9.1%)	(-2.2%)	(-4.3%)
Transformer (other)	2.40±0.00	118.3±0.6	27.3±0.1	1.50±0.00	0.07±0.00	0.27±0.00
	(-1.7%)	(-3.7%)	(-2.2%)	(-4.9%)	(-2.2%)	(-4.3%)
TPC	<b>1.78±0.02</b>	<b>63.5±4.3</b>	<b>21.7±0.5</b>	<b>0.70±0.03</b>	<b>0.27±0.02</b>	<b>0.58±0.01</b>
TPC (labs)	1.85±0.01	72.0±2.2	22.5±0.2	0.81±0.01	0.24±0.01	0.55±0.00
	(-3.9%)	(-13.4%)	(-3.7%)	(-15.7%)	(-4.1%)	(-7.1%)
TPC (other)	<b>1.81±0.02</b>	<b>68.5±4.7</b>	<b>21.8±0.3</b>	<b>0.77±0.03</b>	<b>0.26±0.01</b>	<b>0.57±0.01</b>
	(-1.7%)	(-7.9%)	(-0.5%)	(-10.0%)	(-1.4%)	(-2.4%)

We performed ablations on the type of time series variable that we include: laboratory tests only (labs), which are infrequently sampled, and all other variables (other) which includes vital signs, nurse observations, and automatically recorded variables (e.g. from ventilator machines). This shows how well each model can cope with time series exhibiting different periodicity and sampling frequencies. The results are shown in Table 7.

The TPC model has the largest percentage gain when the labs and other variables are combined (this is synonymous with the greatest percentage impairment in the ablations). Next are the CW LSTM and Transformer, followed by the LSTM. This suggests that the TPC model is best able to exploit EHR time series with different temporal properties.

When examining the results for LSTM and CW LSTM in more detail, we can see that the CW LSTM only has an advantage when the model has to combine the data types. This supports the hypothesis stated in Section A.5 that the CW LSTM is better able to cope when there are varying frequencies in the data, as it can tailor the processing to each. When the inter-feature variability is small (the same type of time series) they perform similarly.

It is unsurprising that the Transformer does better than the LSTM when combining data types, as it can directly skip over large gaps in time to extract a trend in lab values, while simultaneously attending to recent timepoints for the processing of other variables.

The TPC is the most successful model; its inherent periodic structure helps it to extract useful information from all of the variables. The CW LSTM and Transformer do not have this in their architectures, making the derivation more obscure. The importance of periodicity is discussed in more detail in Section 6.



C.2. Loss Function

Table 8. The effect of training with the mean squared logarithmic error (MSLE) loss function when compared to mean squared error (MSE). The metrics are defined in Section B. The colour scheme and confidence interval calculation is described in the legend to Table 1.

Model	MAD	MAPE	MSE	MSLE	$R^2$	Kappa
LSTM (MSLE)	<b>2.39±0.00</b>	<b>118.2±1.1</b>	26.9±0.1	<b>1.47±0.01</b>	0.09±0.00	<b>0.28±0.00</b>
LSTM (MSE)	2.57±0.03	235.2±6.2	<b>24.5±0.2</b>	1.97±0.02	<b>0.17±0.01</b>	<b>0.28±0.01</b>
CW LSTM (MSLE)	<b>2.37±0.00</b>	<b>114.5±0.4</b>	26.6±0.1	<b>1.43±0.00</b>	0.10±0.00	0.30±0.00
CW LSTM (MSE)	2.56±0.01	218.5±4.0	<b>24.2±0.1</b>	1.84±0.02	<b>0.18±0.00</b>	<b>0.34±0.01</b>
Transformer (MSLE)	<b>2.36±0.00</b>	<b>114.1±0.6</b>	26.7±0.1	<b>1.43±0.00</b>	0.09±0.00	<b>0.30±0.00</b>
Transformer (MSE)	2.51±0.01	212.7±5.2	<b>24.7±0.2</b>	1.87±0.03	<b>0.16±0.01</b>	0.28±0.01
TPC (MSLE)	<b>1.78±0.02</b>	<b>63.5±4.3</b>	<b>21.7±0.5</b>	<b>0.70±0.03</b>	<b>0.27±0.02</b>	<b>0.58±0.01</b>
TPC (MSE)	2.21±0.02	154.3±10.1	<b>21.6±0.2</b>	1.80±0.10	<b>0.27±0.01</b>	0.47±0.01